Histol Histopathol (2019) 34: 1025-1036

http://www.hh.um.es

Histology and Histopathology

From Cell Biology to Tissue Engineering

Transcription regulators are transiently expressed during the prostate gland adaptation to the hypoandrogenic environment

Umar Nishan[1], Rafaela Rosa-Ribeiro[1], Carlos Lenz Cesar[2,3] and Hernandes F. Carvalho[1,3]

[1]Department of Structural and Functional Biology, Institute of Biology, [2]Department of Quantum Electronics, Institute of Physics Gleb Wataghin, State University of Campinas (UNICAMP) and [3]INFABiC – National Institute of Science and Technology in Photonics Applied to Cell Biology, Campinas SP, Brazil

Summary. The high incidence of prostatic diseases, including malignant tumors, makes the understanding of prostate biology very important. Androgen deprivation, blockade by orchiectomy, or chemical castration causes prostate and tumor shrinkage. The gene networks involved in a cell type-specific fashion are rather unknown. This work was undertaken to identify genes with annotated function in transcription regulation that might define transitions in gene expression. A total of 15 potential regulatory genes were identified. Validation by qRT-PCR showed that *Zfp703* and *Arid1a* exhibit expression maxima at day 1; *Ash2l, Nelf, Pbx3, Eya2* at day 4; *Dmrt2* at day 5 and *Lbh* and *Sox1* at day 7 after castration. Using immunohistochemistry, we further determined that PBX3 was found in both stromal and epithelial cells, whereas ARID1A and NELF were restricted to the epithelium, and DMRT2 and EYA2 were exclusively found in the stroma. Though the proteins ZFP703 and ASH2l were not found in any experimental condition, their mRNAs were located by *in situ* hybridization in both epithelium and stroma. In conclusion, androgen deprivation triggers the expression of temporally regulated gene sets in both epithelial and stromal cells. These gene subsets will help establish the regulatory gene expression programs orchestrating the castration-induced remodeling of the prostate gland, and represent putative targets to increase the efficacy of androgen-deprivation to induce epithelial (and cancer) cell death.

Key words: Castration, Prostate, Stroma, Transcription factors, Tissue remodeling

Offprint requests to: Hernandes F. Carvalho, Institute of Biology, Unicamp, Rua Charles Darwin, sn, Bloco N, Salas 10/11, 13083-863 Campinas SP, Brazil. e-mail hern@unicamp.br

DOI: 10.14670/HH-18-105

Introduction

Prostate cancer (PC) is the second leading cause of cancer deaths in men, afflicting mostly the elderly. A significant fraction of these men receive androgen ablation by either surgical or chemical castration for the treatment of the advanced disease and most of them will die after progression of the disease to the more aggressive and life threatening form, described by the general term castration-resistant prostate cancer (CRPC). Many molecular and chromosomal changes are associated with PC, such as frequent rearrangements within chromosome 21 (Tomlins et al., 2005). The chromosomal rearrangements include the TMPRSS2:ERG fusion gene, in particular, as well as other androgen regulated genes at the 5' end, and different ETS genes at the 3' end of the fused construction, and occasionally replaced by BRAF or RAF, as non-ETS members (Palanisamy et al., 2010). More recently, generalized chromosomal rearrangements have been described (Baca et al., 2013). Progress has also been achieved in the demonstration of the clonal progression to metastasis (Haffner et al., 2013), with particular efforts resulting in a clear demonstration of patient specific variation in gene expression, rather than

showing an expected signature related to metastasis (Holcomb et al., 2009).

On the other hand, less is known of the mechanism leading to CRPC. It is certainly dependent on modifications of androgen receptor (AR) sensibility and responsiveness, resulting from different in-frame deletions within the gene, amplification, and altered crosstalk with other signaling pathways, along with modifications in the metabolic pathways to produce androgens (Feldman and Feldman, 2001; Nyquist et al., 2013; Yuan et al., 2014). In spite of the assumption that androgen deprivation results in selection of androgen-independent subpopulations in the tumor, it is difficult to ascertain whether any particular alteration is already present at the beginning of androgen deprivation therapy. The physiology of the prostate gland's adaptation to the hypoandrogenic environment promoted by castration is still poorly understood. In addition, the effects of androgen deprivation on blocking cell proliferation and promoting cell death have been definitively shown as distinct events taking place at different androgen levels (Isaacs, 1984). Progress in identifying regulators of cell cycle progression in both PC and CRPC using cell models revealed new avenues for the use of cytostatic compounds in either case, such as PI3K/AKT and/or mTOR inhibitors and blockers of AR ancillary factors, such as GATA2 (Sunkel and Wang, 2014) .

The cell death response in the epithelium after castration has been unequivocally demonstrated to be independent of the AR (Kurita et al., 2001), but the mechanism leading to epithelial cell apoptosis is unknown. This suggests the existence of an underlying regulatory network, triggered by androgen deprivation and taking place in the hypoandrogenic environment, but not directly dependent on AR function. Nonetheless, we have reported before that epithelial desquamation (not involving apoptosis) also contributes to cell deletion after castration (Rosa-Ribeiro et al., 2014a) and that a protease-dependent wave of apoptosis occurs at day 11 after castration (Bruni-Cardoso et al., 2010). These two phenomena are distinct from the apoptosis occurring 3 days after castration.

We have hypothesized that among genes that show the typical pattern of being stimulated or repressed by testosterone/dihydrotestosterone stimulation via the androgen receptor and, hence, repressed or upregulated after castration, respectively, there would exist genes involved with coordinating the many phenomena taking place after castration, including those setting the new transcriptional states characteristic of the new cell identities. In particular, the functioning of a subpopulation of macrophages seems relevant to preserve a non-inflammatory environment (Silva et al., 2018). Furthermore, our own transcriptome and bioinformatics study revealed a number of transcription factors and transcription regulators regulating cell survival, proliferation, and a new 'immature signature" (Rosa-Ribeiro et al., 2014b). Of note, we found NFκB family members, MYBL2, EVI1, ELK1, and NFY as important players.

One limiting factor in the analysis of microarray data is the incompleteness of information about the investigated genes, which depend upon the available information at the time of the investigation, and on continuously evolving data banks and search software, as well as careful annotation. One specific limitation of mining published lists of differentially expressed genes is shown by the ratio between known genes and expression tags (EST). The report by Desai et al. (2004) revealed 1496 differentially expressed transcripts in the ventral lobe of the prostate gland (VP), 32% of them were named genes.

This work is part of our efforts to build up a coherent sequence of regulatory steps coordinating the different phenomena occurring after castration. To overcome the intrinsic limitation of automatic gene identifier tools, we manually searched the microarray data set for genes with expression transients at days 1, 3, 5, or 7 after castration, determined their identity and then validated the expression of 15 such genes by quantitative real time PCR. We also considered that those genes could be restricted to expression in particular cell types within the organ, and thus used either immunohistochemistry or *in situ* hybridization to determine the expression location of seven of them in the organ. The results revealed the kinetics of transiently expressed gene subsets in both the epithelium and the stroma of the prostate gland following castration, and their distribution within the gland, and identified two nuclear factors (NELF and ARID1A) contributing the transcriptional identity of the epithelium.

Materials and methods

Methodology for gene identification and selection

In previous work we used DAVID to determine gene identities and further explore the microarray data from Desai et al. (2004), in a search for TF/TR. However, only 32% of the genes were automatically retrieved and we thought that important data could be still embedded in the remaining ESTs. We then searched the remaining non-identified ETS for differentially expressed genes with peak variation at days 1, 3, 5, or 7 after castration, and subsequently used the NCBI databank to correlate the transcripts with their corresponding genes and then searched for their annotated functions. A list of 15 transcription factors or transcription regulators was retrieved. These genes were then validated by RT-PCR and 7 of them showed transient expression and were subsequently studied by immunohistochemistry or *in situ* hybridization for identification of the gland compartment or cell type distribution.

Animals

We used 90-day-old male Wistar rats (n=56, weighing 380±20 g), with free access to food and water,

in this study. Castration was achieved by bilateral orchiectomy through a scrotal incision under ketamine hydrochloride (80 mg/kg) and xylazine hydrochloride (10 mg/kg) anesthesia. The animals were separated into 8 experimental groups (seven animals per group). Each group of seven animals was divided into 2 subgroups i.e. 3 animals for morphology and related studies and 4 animals for RNA and protein extraction. The 2 lobules of the gland were separated and each used for RNA or protein extraction. An additional 8 rats were used for *in situ* hybridization experiments, increasing the total number of animals employed in this work to 64. The experimental design, including sample size and procedures, was approved by the State University of Campinas Committee on the Use of Animals (Protocol 3000-1), according to the Brazilian College for Animal Experimentation.

Prostate sample collection

Eppendorf tubes for the collection of ventral prostate samples for RNA extraction were pre-treated with H_2O_2. Ventral prostate samples were fixed in 4% para-formaldehyde (PFA) in phosphate buffered saline (PBS) for the morphological studies. The volume of the PFA solution used was approximately 30 times the total volume of the tissue fragments. For RNA and protein extraction, the samples were immediately frozen in liquid nitrogen and stored at -80°C until used.

RNA extraction and reverse transcription

Ventral prostates were dissected under RNAse free conditions. Thirty mg of tissue was used for total RNA extraction. Subsequently, the tissue fragments were extracted using Illustra RNAspin Mini Kits (GE Healthcare, Germany) according to the manufacturer's instructions. RNA purity was analyzed by the absorbance ratio 260/280 (values higher than 1.8) and by electrophoresis in 1.2% agarose gel under denaturing conditions. The RNA concentration in each sample was determined in an Ultraspec 2100pro spectrophotometer (Amersham Biosciences). Next, 5 µg of total RNA was reverse transcribed with 200 U SuperScript III (Invitrogen Corporation) and oligo $(dT)_{12-18}$ primer (Invitrogen Corporation), according to the manufacturer instructions. cDNA was quantified by spectro-photometry.

Quantitative real time PCR (qRT-PCR)

Quantitative real-time polymerase chain reaction (qRT–PCR) was performed using TaqMan Universal PCR Master Mix (Applied Biosystems, Foster City, CA) in the Applied Biosystems 7300. Inventoried assays (Primer and FAM-conjugated probes) listed in Table 1, were purchased from Applied Biosystems. cDNA (20 ng) was used in each reaction, according to universal cycling conditions for the TaqMan system. The results were normalized using the CT (threshold cycle) values of the internal control glyceraldehyde-3-phosphate dehydrogenase (*Gapdh*) on the same plates. *Gapdh* was chosen as internal control because it was found to show the least standard deviation among the experimental groups after testing 9 other controls for this specific purpose. The equation $\Delta CT = C_T$ (target gene) - C_T (internal control) was employed for normalization of the results. In order to quantify and acquire the fold-change variation of our genes the mathematical model $2^{-\Delta\Delta CT}$ was utilized. Our genes and *Gapdh* assays had their efficiencies calculated through the equation: $E=10^{(-1/slope)}$. All reactions were performed in technical triplicates and the experiment was repeated twice.

Immunohistochemistry

PFA-fixed, paraffin-embedded tissues were cut into 5 µm sections, mounted on silane-treated slides, dewaxed in xylene, and rehydrated. The sections were briefly treated in a microwave oven in 10 mM citrate buffer pH 6.0, then blocked with 3% H_2O_2 for 10 min, followed by incubation with 6% bovine serum albumin for 1 h. The sections were incubated overnight with antibodies from Abcam or Thermo-Scientific diluted 1:1000 (DMRT2), 1:500 (for NELF), or 1:100 (for ZNF703, ASH2L, ARID1A, EYA2 and PBX3). The tissue-bound primary antibody was detected with a 488 Alexafluor-conjugated goat anti-rabbit Ig (Invitrogen Carlsbad, CA, USA). Samples were analyzed in a Leica 750 fluorescence microscopy and the images captured with a CCD camera.

In situ mRNA hybridization

For mRNA localization, all solutions and materials utilized were RNAse free. The probes were designed using the Gene Runner 3.05 software (Hastings Software, Inc., USA) according to mRNA sequences in NCBI NM_001109425 and BF548399 for *Zfp703* and *Ash2l*, respectively. Two probes were synthesized for each mRNA and were 5'-end labeled with Alexafluor 488 by Invitrogen Life Technologies (Carlsbad CA, USA). Both sense and antisense sequences are given in Table 2.

Frozen sections were air dried for 30 min at 37°C, fixed in 4% PFA for 5 min, and washed in PBS twice for 5 min and twice in 2X SSC for 2 min. The sections were incubated with Proteinase K (20 µg/mL) for 10 min at room temperature and then washed twice for 5 min with 2x SSC buffer. The sections were incubated in 0.1 M triethanolamine pH 8 (TEA Buffer) for 10 min and then with 0.25% acetic anhydride in TEA buffer for 10 min under magnetic stirring and then washed with 2x SSC. The pre-hybridization solution was composed of 50% formamide, 5x SSC, Denhardt's solution (1x final concentration), and completed with DEPC-treated water. The sections were prehybridized for 3 hours without the probe at 50°C in a humidified chamber with 50%

formamide in SSPE. The probe mix included the probes for each Zfp703 or Ash2l mRNAs and consisted of pre-hybridization solution plus 400 ng of torula RNA and 200 ng of riboprobe mix (anti-sense or sense) (100 μL for each tissue section). The mixture was placed on the sections and incubated at 50°C overnight in a humidified chamber. After 24 hours hybridization, the sections were washed four times with 4x SSC buffer for 10 in PBS. The sections were visualized with a Zeiss LSM780 confocal microscope.

Table 1. Gene names, accession numbers, sequences of reverse and forward primers, probes and the average melting temperature of the primers used in the current study.

S.No	Gene Name	Accession No	Primer/Gene Code	Sequence	Average Melting Temperature(Tm) °C
1	Zinc finger protein 703	NM_001109425	Znf703_F	TGGTGGCTGGAGGTCTTGAG	63.6
			Znf703_R	GCGGGTTGTTTTTGTGGAGTA	
			Znf703_P	AGAATTCTGTTGTGCTGTGTG	---
2	Absent, small or homeotic-like (Drosophila)	BF548399	Ash2_F	AGGGTGTGGCTTACAAGGATATTT	62.2
			Ash2_R	CGTGCAGCTCTTGTACAGTGAGA	
			Ash2_P	TGAAGGTGTTTACTTCCCAG	---
3	Basic helix-loop-helix transcription factor	NM_021592	bLHL_F	CTCTCGCTGCCTACAGAAACCT	63.45
			bLHL_R	CAAGGCTGGAGATGACACGAA	
			bLHL_P	CAAGAAGTCCGCAGGTC	---
4	D site of albumin promoter (albumin D-box) binding protein	NM_012543	Dbp_F	GCAGCCAAGAGGTCGAGAGA	64.15
			Dbp_R	AGGCTGCCCGCACAGAT	
			Dbp_P	AAGACTCAAGGAGAACCAGA	---
5	Nelf nasal embryonic factor	AJ293697	Nelf_F	GGAGAGGAAGCGTCGGAAAC	63.35
			Nelf_R	TGCGGAAGTTCCTCTGGATT	
			Nelf_P	AGAATGATTCCGCGTCTG	---
6	Similar to limb-bud and heart	AA800701	Loc683626_F	CCCCTGACCTGCTCAGACA	63.7
			Loc683626_R	GGGTGGCTTCTTCCTTTTGC	
			Loc683626_P	TTGTACAACATGGTCTAGTGAC	---
7	Pre-B-cell leukemia homeobox 3	BF398712	Pbx3_F	CACGGTCAAACCCCAGACA	63.15
			Pbx3_R	TTGCCCTGAGATGAAGATCTTG	
			Pbx3_P	TCTTGTTTTCACCTCTGTAGC	---
8	Eyes absent homolog 2 (Drosophila)	AW918854	Eya2_F	GAGCAAGGAGCCAAAAAGCA	62.95
			Eya2_R	AGGTCAGCGTGGCAGGATAT	
			Eya2_P	AACATGCCGTTCTGGAG	---
9	Zinc finger protein 219	BE105452	zfp219_F	TCCTTAACAGCAGCACATCCTCTAC	62.9
			zfp219_R	GGCAGAGGTGAGGGTCAAAG	
			zfp219_P	AGCCCTAGGACCCCGT	---
10	SRY (sex determining region Y)-box 17	BF551118	Sox17_F	GGGTTTGCTCCCCACCAT	63.05
			Sox17_R	TTTCTTTGGATCAAGTTGGTGAGAT	
			Sox17_P	ACTGTCCAGTTTTAGCCAGT	---
11	LIM and cysteine-rich domains 1	AW919666	12-Lmcd_F	GCCTGCTGATGGACTCCAA	63.35
			Lmcd_R	ATGCCGTCTCCACCTTTCAC	
			Lmcd_P	TATGCCACTCTTACTGCCAG	---
12	Double sex and mab-3 related transcription factor 2	AW918208	Dmrt2_F	CGGAATTTGTCCCCCATTG	63.6
			Dmrt2_R	TTGGTTAAGACGTGCCCTTGA	
			Dmrt2_P	TGATATGGACTGTCTGGCAG	---
13	High mobility group box 1	BE107162	Hmgb1_F	AAAACCCACAAAATTGCCAAA	61.75
			Hmgb1_R	CCCGAACTCATTCATTAATCATGTT	
			Hmgb1_P	TGTTCCCTAAACTAAGCAGAT	---
14	Treacher Collins-Franceschetti syndrome 1 homolog (human)	BE108177	Tcof1_F	AGCAGTTCTGTCAGGACCTTCAT	63.4
			Tcof1_R	CCCTGGCCCCTGAGTGA	
			Tcof1_P	ACAGAGGCCTGCACC	---
15	AT rich interactive domain 1A (SWI-like)	AW536019	Arid1a_F	CAAAGCGAGACACAGCTATTTAATCT	61.95
			Arid1a_R	CCTGTAGAGCATCGCACCAA	
			Arid1a_P	TTGCCAGACGTCGCC	---
16	Zinc finger protein 142	BE101212	znf142_F	GGTGGTCACTGGAGATTCAGTCA	63.05
			znf142_R	GGCTTGGACTAAACCATTGATTTC	
			znf142_P	AGGTCAAACCATAACACTAC	---
17	Similar to Forkhead box protein F1	AA817785	FKHK5_F	ATACCCTCAGACTGTCCCTTTGAT	61.65
			FKHK5_R	CGGCATCTGTGACACATATTTTAAA	
			FKHK5_P	CAGTGCAGAAAGGAG	---

Statistical analyses

Data are reported as the mean ± standard deviation (SD). Differences between groups were determined by one-way analysis of variance (ANOVA), followed by the post hoc Tukey's test. Differences were considered to be significant when $p \leq 0.05$. Experiments were performed in triplicate.

Results

Identification of new TF and TR differentially expressed in the rat ventral prostate after castration

In this work, we have extended our search by manually identifying mRNAs with transient expression at days 1, 3, or 5 after castration, or with an expression maximum at day 7, and then selected those with annotated TF or TR function, or had homologies to known TF or TR in other species. This search retrieved 15 new genes, which were further validated by qRT-PCR.

mRNA levels for the selected genes at different time points after castration

Castration promoted a marked reduction in ventral prostate weight. Seven days after surgery, the organ was reduced to about 33% of its original size. There was a small increase in the relative weight of the gland 24-28 hours after castration, which has been observed before (Garcia-Florez et al., 2005; Bruni-Cardoso et al., 2010) and was attributed to initial edema, possibly due to increased blood vessel permeability (Shabsigh et al., 1998).

We have collected the ventral prostate from these samples for mRNA extraction and qRT-PCR determination of their content variation, daily up to 7 days after castration.

qRT-PCR was performed for all of the selected genes using probes and primers mentioned in Table 1. The results showed several patterns of expression variation after castration, considering their changes in expression along time (Fig. 1). Of the genes, 7 of them (*Znf703, Ash2l, Nelf, Pbx3, Eya2, Dmrt2,* and *Arid1a*) showed the expected transiently increased expression after castration and were further studied by immunohistochemistry for the determination of their location in either prostate epithelium and/or stroma.

Location of the proteins in the gland

Of the 15 selected genes, 7 were confirmed to have transient expression within the first week after castration and were further analyzed with respect to their compartmentalization in the prostate gland. Fig. 2 shows the representative IHC results for these eight TFs.

DMRT2 showed a very restricted distribution 5 days after castration in stromal fibroblast-like cells (Fig. 2a). Immunohistochemistry for DMRT2, at 6 and 7 days after

Table 2. Sequences of probes for *in situ* hybridization.

Name of Factor	Accession #		Sequence of probe
Znf703	BE101212	Sense 1	5' CATCCTCTCTACACCTATGGCTTCATGCTG
		Antisense 1	5' CAGCATGAAGCCATAGGTGTAGAGAGGATG
		Sense 2	5' TTGTTTGGTTTGGACTGATTTGGTATTGAG
		Antisense 2	5' CTCAATACCAAATCAGTCCAAACCAAACAA
Ash2	AW918208	Sense 1	5' TTCAAATACCCTCCAAAGGACGTCACT
		Antisense 1	5' AGTGACGTCCTTTGGAGGGTATTTGAA
		Sense 2	5' GATCCATGCTTCTTATGACATTGTGAAAT
		Antisense 2	5' ATTTCACAATGTCATAAGAAGCATGGATC

Table 3. Summary of the major findings.

Name of Factor	Transcript accession code	Day of peak expression after castration	Fold- change	Gene Product in Epithelial Cells	Gene Product in Stromal cells
Arid1a	AW536019	1	1.4	+	-
Ash2l*	BF548399	4	4.5	+	+
Dmrt2	AW918208	5	2.5	-	+
Eya2	AW918854	4	1.4	-	+
Nelf	AJ293697	4	2	+	-
Pbx3	BF398712	4	1.8	+	+
Znf703*	NM_001109425	1-4	3	+	+

*mRNA has been shown by *In Situ* hybridization in tissue.

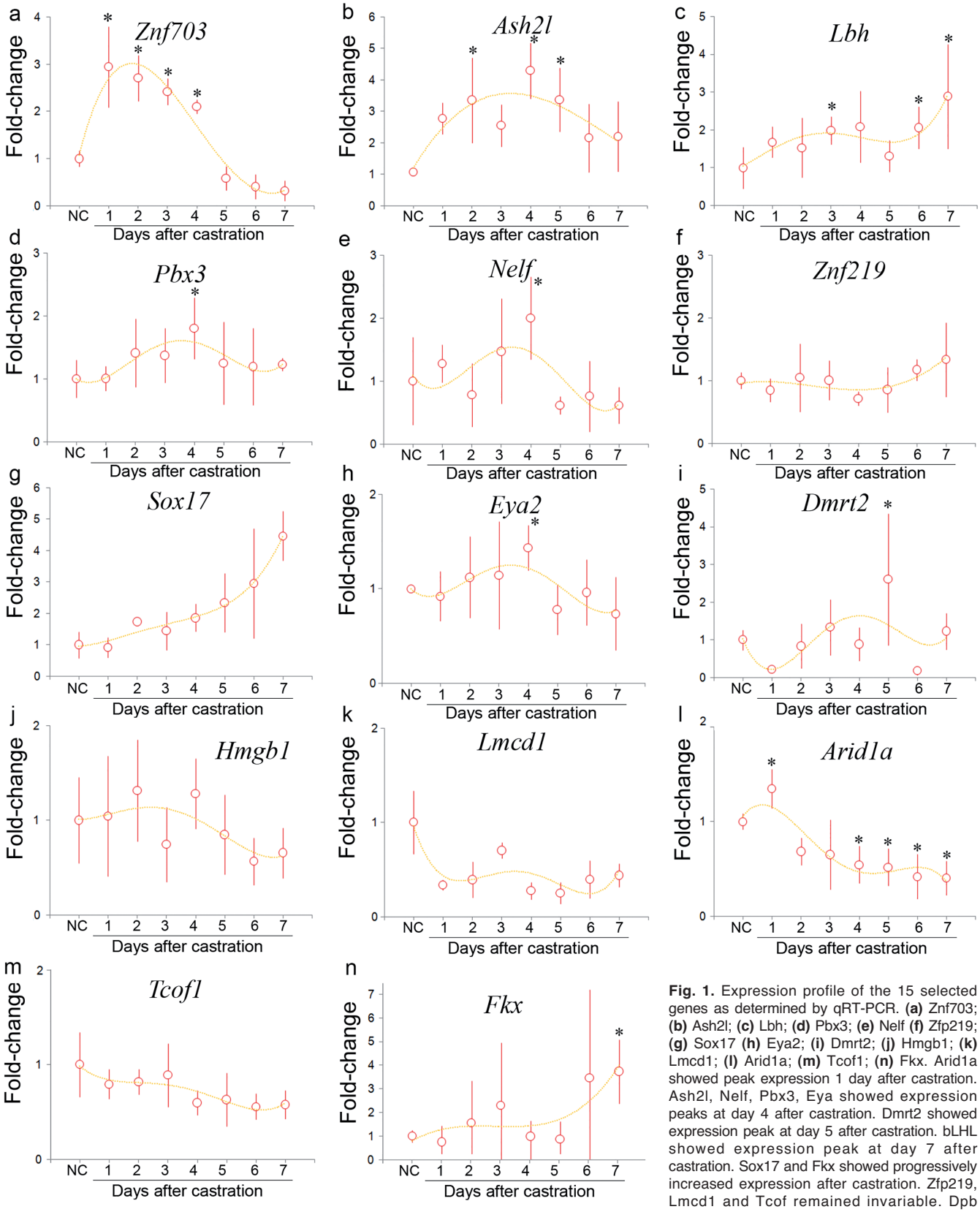

Fig. 1. Expression profile of the 15 selected genes as determined by qRT-PCR. **(a)** Znf703; **(b)** Ash2l; **(c)** Lbh; **(d)** Pbx3; **(e)** Nelf **(f)** Zfp219; **(g)** Sox17 **(h)** Eya2; **(i)** Dmrt2; **(j)** Hmgb1; **(k)** Lmcd1; **(l)** Arid1a; **(m)** Tcof1; **(n)** Fkx. Arid1a showed peak expression 1 day after castration. Ash2l, Nelf, Pbx3, Eya showed expression peaks at day 4 after castration. Dmrt2 showed expression peak at day 5 after castration. bLHL showed expression peak at day 7 after castration. Sox17 and Fkx showed progressively increased expression after castration. Zfp219, Lmcd1 and Tcof remained invariable. Dpb showed an oscillatory expression pattern. Data are expressed as the mean ± SD (n=3). * is showing statistical difference among the groups.

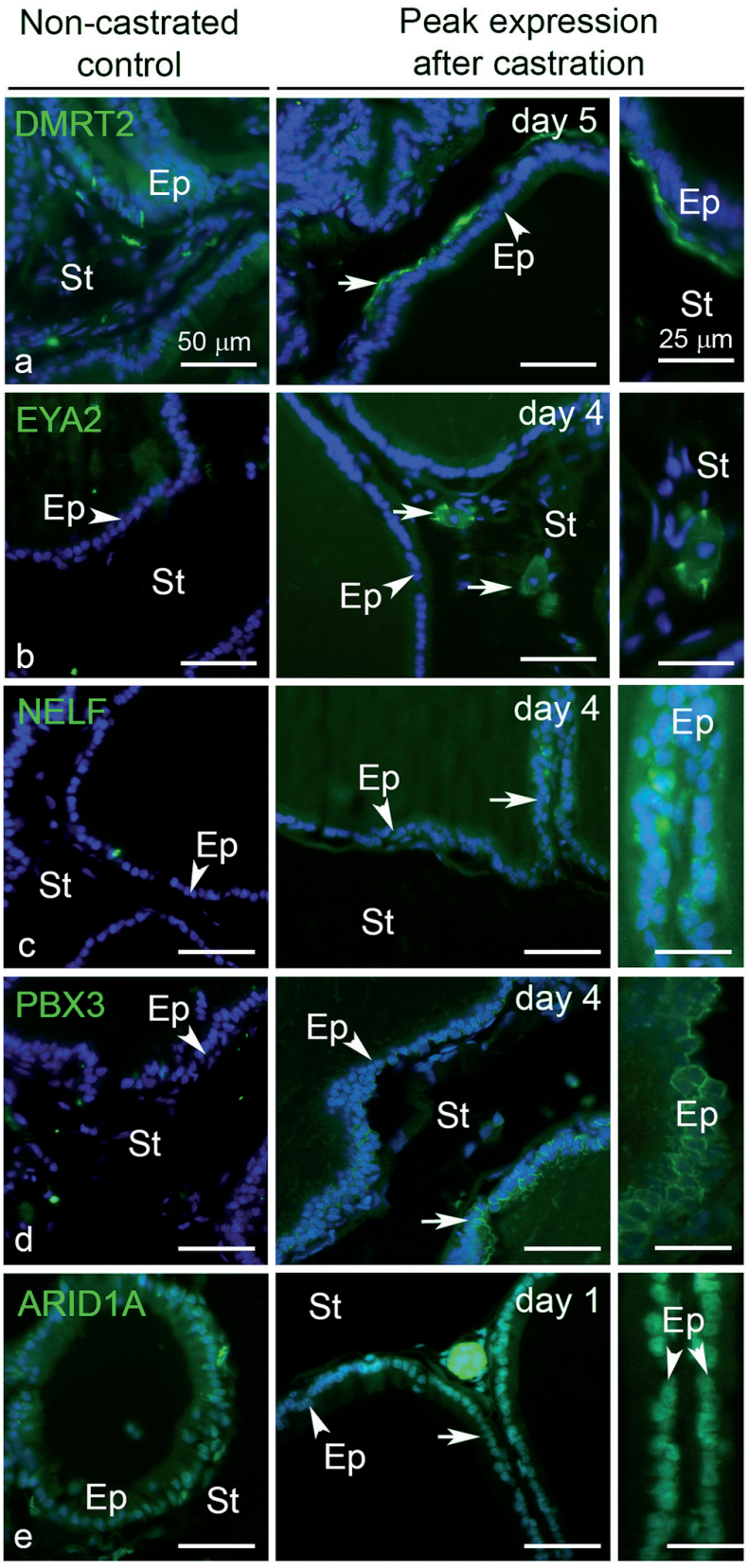

Fig. 2. Immunohistochemical localization of ZNF142, DMRT2 **(a),** EYA2 **(b)**, NELF **(c)**, PBX3 **(d)**, and ARID1A **(e)** in the rat ventral prostate of non-castrated controls and at the day of peak expression. **a.** Little staining for DMRT2 was found in non-castrated controls (left). The arrows show a fibroblast-like cell, showing expression of DMRT2 5 days after castration (middle), which is seen in the detail (right). **b.** No staining for EYA2 was observed in non-castrated control (left), while large stromal cells expressing EYA2 were found 4 days after castration (arrows in the middle panel). A detail of these cells is shown in the right panel. **c.** The non-castrated controls showed very faint labeling for NELF (left), while staining appeared increased 4 days after castration in the epithelial cells and showed a slight accumulation in the nuclei of the epithelial cells (middle panel and detail in the right). **d.** PBX3 labeling was absent in the non-castrated controls (left), while it was found in both the epithelial and stromal cells 4 days after castration (middle). In particular, the staining was associated at the cell membrane, and showed clear distribution along the cell perimeter (detail in the right panel). **e.** ARID1A labeling was seen in the non-castrated control epithelium and was predominantly located in the cytoplasm (left). After castration it was predominantly found in the cell nucleus (middle panel and detail in the right). Ep: epithelium; St: stroma. Scale bars: 50 µm in the overall views and 25 µm in the details.

castration, showed no staining. EYA2 was located in stromal cells 4 days after castration exclusively (Fig. 2b). A very faint staining for NELF was observed in the epithelial cells 4 days after castration, and no expression was observed in the control sample (Fig. 2c). PBX3 was located in both epithelial and stromal cells 4 days after castration, whereas only a very weak staining was visible in the control samples, with a clear association with the cell periphery (Fig. 2d). ARID1A was found in the epithelium of both non-castrated controls and 1 day after castration (Fig. 2e). Immunostaining vanished at days 3 and 4 after castration.

Location of Znf703 and Ash2l mRNAs in the gland

Znf703 and *Ash2l* showed the expected transient

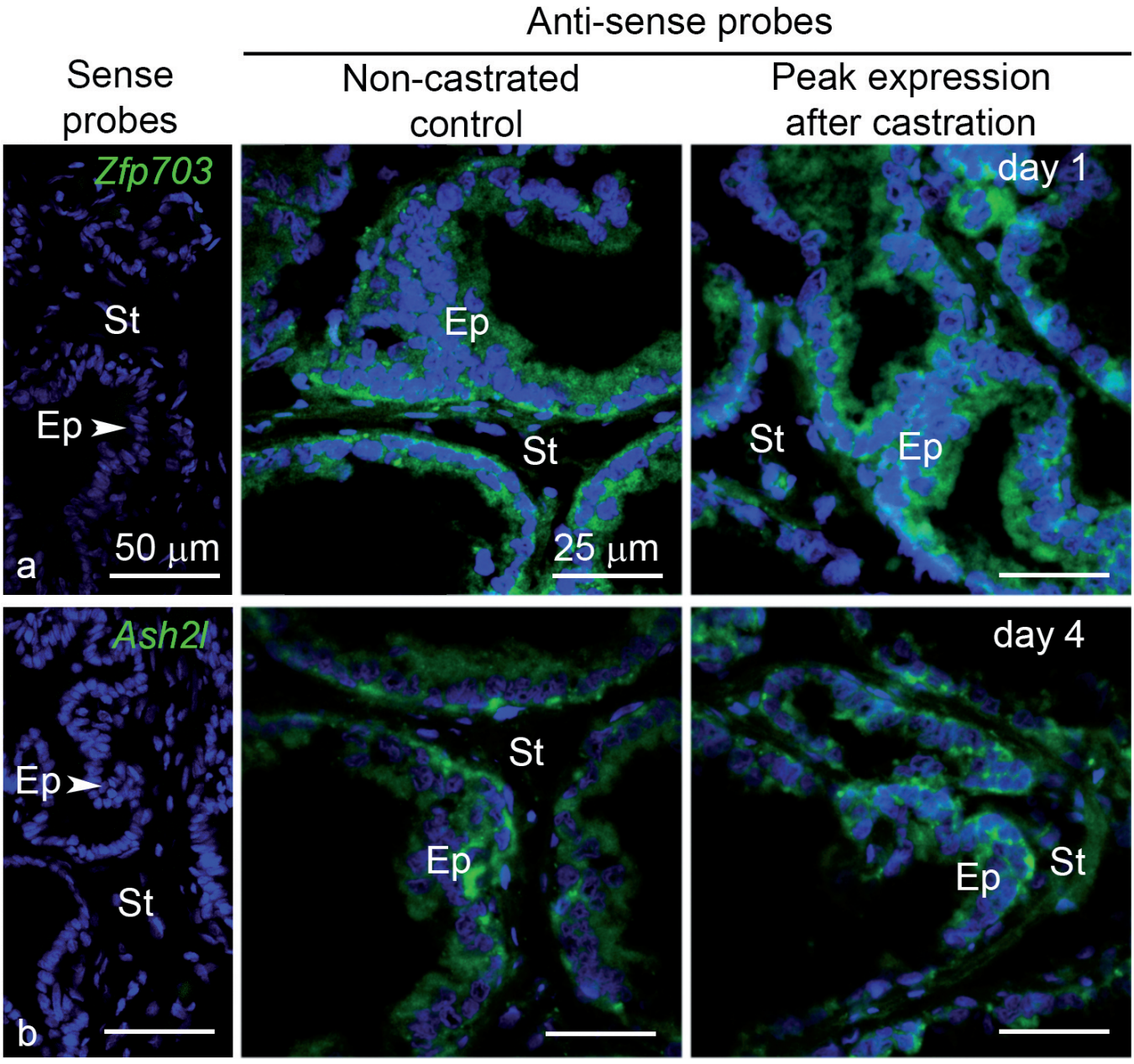

Fig. 3. *In situ* hybridization for the localization of Znf703 **(a)** and Ash2l mRNAs **(b)** in non-castrated controls (middle panels) and in castrated animals at the day of peak expression (day 1 for Znf703 and day 4 for Ash2l (right panels). Sense probes were used as negative controls (left panels). Hybridization with anti-sense probes was found in both epithelium and stroma for Znf703 and Ash2l mRNAs. Scale bars: 25 μm in the middle and right panels and 50 μm in the negative controls (left panels).

kinetics after castration, but could not be found at the protein level using either immunohistochemistry or western blotting. It is important to mention that the antibodies employed here could identify each protein in a positive control or in the neonatal prostate (Nishan et al., 2015). To identify *Znf703* and *Ash2l* transcripts within the gland, we performed *in situ* hybridization. The results showed the presence of both *Znf703* and *Ash2l* mRNAs in the epithelium and stroma in the non-castrated controls as well as in castrated animals at day 1 for *Znf703*, and day 4 for *Ash2l* (Fig. 3).

Results are summarized in Table 3.

Discussion

Using qRT-PCR, we have determined the variation in mRNA levels for 15 genes manually selected from the results by Desai et al. (2004) and found 7 of them to show transient increases within the first week after castration. The products for these 7 genes were located in the gland, and subsets were determined to be located in either the epithelium or stroma. ARID1A and NELF were found exclusively in the epithelium, whereas EYA2 and DMRT2 were restricted to stromal cells and ZNF703, ASH2L, and PBX3 were found in both compartments (Table 1).

The prostate gland is highly dependent on androgens for its development, growth, and functioning and castration promotes the active and progressive inactivation of the gland (Isaacs, 1984; Kyprianou and Isaacs, 1988; Isaacs et al., 1994). The current study showed a 67% reduction in the weight of VP 7 days after castration, which was consistent with previous quantification in the same system (Bruni-Cardoso et al., 2010). Analyses of long-term (100 days) androgen deprivation showed that the organ shrank to about 5% of the prostate weight in age-matched control animals (Antonioli et al., 2007).

However, the prostate adaptation to the hypoandrogenic environment is complex. This complexity reflects the ability of the organ to adjust its activity to the overall reproductive function, which is particularly evident in seasonal breeders and/or in species with social male hierarchy. While the major factors controlling these variations, such as light-dark cycles, temperature, and food availability in the former and unknown factors in the latter, androgens are chief executives of gland activity. Accordingly, in a previous study, the authors found a series of circadian rhythm genes differentially expressed after castration (*Bmal1, Clock, Per2* and *Nr1d1*) (Kawamura et al., 2014).

In an apparent paradox, and perhaps appearing as a manifestation of the existence of a refined and yet ill-known physiological control, prostate epithelial cell death occurring after castration is dissociated from the central mastery of androgen signaling. This was indicated by the fact that cell death was independent of the expression of AR in the epithelial cells (Kurita et al., 2001), as well as by the notable differences between the ventral and dorso-lateral lobes of the rodent prostate, characterized by reduced levels of apoptosis and the relative scarcity of genes affected by castration in the dorso-lateral lobes, as compared with the ventral lobes (Kwong et al., 1999; Desai et al., 2004).

These differences are indicative that hidden mechanisms are imperative for adjusting the gland to varying levels of circulating androgens. More recently, insights into these mechanisms have been appearing, as new transcription factors are enrolled in the observed cell and extracellular matrix changes (Sunkel and Wang, 2014; Rosa-Ribeiro et al., 2014b). Additional layers of AR regulation have been reported for cultured cells, including the transcription factors GATA2, FoxA1, and MED1-dependent DNA loop formation (Sunkel and Wang, 2014), while NFkB family members, MYBL1/2, EVI-1 among others reveal a "transcription factor signature", characterizing the new epithelial and stromal cell identities in the hypoandrogenic environment (Rosa-Ribeiro et al., 2014b).

In general, reports in the literature about the 7 genes identified here are scarce, providing exciting opportunities.

Dmrt2 is expressed in presomitic mesoderm and developing somites (Kim et al., 2003). In our study, it showed the expected expression profile with peak expression 5 days after castration. The Dmrt2 protein was found 5 days after castration in fibroblast-like cells, suggesting that stroma-specific regulatory networks are active after castration.

Eyes absent homolog (EYA) proteins play pivotal roles in organ formation during development by interacting with Sine Oculis (SO) and Dachshund (DAC) (Jung et al., 2010). Drosophila eyes absent homologue 2 (EYA2) in *Drosophila* is a conserved transcriptional regulator (Zhang et al., 2005). Furthermore, loss-of-function mutants cause partial or complete absence of the compound eye. Eya2 triggers rapid apoptosis in interleukin-3 dependent 32D.3 murine myeloid cells (Wesley-Clark et al., 2002). Consistent with previous studies on the expression profile of Eya2, the identified expression pattern suggests *Eya2* to be a master switch regulatory gene in the adult prostate with peak expression four days after castration. Considering that Eya2 protein expression was located by immunohistochemistry in the stromal cells after castration, it is unlikely to be a direct regulator of epithelial apoptosis.

Nelf is a guidance molecule for olfactory axon projections and neurophilic migration of luteinizing hormone releasing hormone cells (LHRH) (Kramer and Wray, 2000). LHRH regulates developmental migration and projection of gonadotropin releasing hormone (GnRH3) neurons in zebrafish (Palevitch et al., 2009). Its function in the prostate is largely unknown and demands further studies.

PBX3 is another TF with an expression profile showing peak expression 4 days after castration. *Pbx3* is expressed in both stroma and epithelium 4 days after

castration and seems to be involved in the various structural and physiological changes that take place after castration. *Pbx3* has been reported to be up-regulated in prostate cancer and post-transcriptionally regulated by androgen through Let-7d, an androgen regulated microRNA (Ramberg et al., 2011).

Arid1a is part of the SWI/SNF chromatin-remodeling complex. ARID1A has been reported as a tumor suppressor (Jones et al., 2010). It showed a transient increase 1 day after castration. As determined by immunohistochemistry, ARID1A was found in a few acini in both non-castrated control and castrated rats 1 day after surgery. Moreover, 2 days after castration, we found a small number of cells expressing ARID1A, but no staining was found 3 or 4 days after castration. This TF seems to take part in the very early response to castration, which, in association with its localized expression in the gland of non-castrated animals, reveals a possible association with transitions in chromatin activity and makes ARID1A an interesting candidate for further studies.

ZNF703 is a transcriptional repressor (Nakamura et al., 2008) and a key regulator of breast cancer progression (Slorach et al., 2011). *Znf703* induces cell proliferation and interferes with the TGFβ pathway. In MCF7 cells, increased ZNF703 expression results in activation of genes involved in stem cell self-renewal, while in primary human mammary epithelial cells, ZNF703 increases the ratio of luminal to basal progenitors. ZNF703 over expression was also shown to alter the regulation of proliferation and differentiation in luminal breast tumors (Bazarov and Yaswen, 2011). Our results show that *Znf703* expression increased transiently by days 1-4 after castration and that the mRNA was found in both epithelium and stroma. These findings suggest that ZNF703 is either present below the limit of detection by immunohistochemistry or immediately degraded after translation, a possibility that needs to be checked experimentally. It will be interesting to determine whether ZNF703 is necessary for any active movement within the epithelial layer early after castration that might be associated with the reorganization of the basement membrane we reported before (Carvalho and Line, 1996).

The absent small and homeotic (*Ash2l*) gene is a member of the trithorax group of positive transcriptional regulators of the homeotic genes (Amorós et al., 2002; Cheng and Shearn, 2004). It showed a transient expression profile with peak expression at day 4 after castration. The approximately 4-fold change 4 days after castration led us to speculate that ASH2L may have a pivotal role in the cellular adaptation to androgen deprivation. We could not localize the cells expressing ASH2L in the tissue by immunohistochemistry, though we could detect it in newborn prostate and in cultured smooth muscle cells (results not shown). By *in situ* hybridization we managed to determine the distribution of mRNA in both non-castrated control and castrated rats 4 days after surgery. These results from qRT-PCR and *in situ* hybridization suggest that either ASH2L protein is rapidly degraded after its translation, or it might play some role as RNA.

In conclusion, we report the existence of epithelial and stromal subsets of transiently expressed genes in the prostate within the first week after castration. These genes are poorly known and additional studies will help to determine their function and will translate into potentially druggable targets to approach specifically the transition to the castration-resistant state of the human disease, as well as contribute to identify regulatory circuits downstream of AR activity (Nantermet et al., 2004).

Acknowledgements. U.N. was recipient of a TWAS/CNPq fellowship. This work was funded by a grant from FAPESP (Grant 2009/16150-6).

References

Amorós M., Corominas M., Deák P. and Serras F. (2002). The ash2 gene is involved in Drosophila wing development. Int. J. Dev. Biol. 46, 321-324.

Antonioli E., Cardoso A.B. and Carvalho H.F. (2007). Effects of long-term castration on the smooth muscle cell phenotype of the rat ventral prostate. J. Androl. 28, 777-783.

Baca S.C., Prandi D., Lawrence M.S., Mosquera J.M., Romanel A., Drier Y., Park K., Kitabayashi N., MacDonald T.Y., Ghandi M., Van Allen E., Kryukov G. V., Sboner A., Theurillat J.P., Soong T.D., Nickerson E., Auclair D., Tewari A., Beltran H., Onofrio R.C., Boysen G., Guiducci C., Barbieri C.E., Cibulskis K., Sivachenko A., Carter S.L., Saksena G., Voet D., Ramos A.H., Winckler W., Cipicchio M., Ardlie K., Kantoff P.W., Berger M.F., Gabriel S.B., Golub T.R., Meyerson M., Lander E.S., Elemento O., Getz G., Demichelis F., Rubin M.A. and Garraway L.A. (2013). Punctuated evolution of prostate cancer genomes. Cell 153, 666-677.

Bazarov A.V. and Yaswen P. (2011). Who is in the driver's seat in 8p12 amplifications? ZNF703 in luminal B breast tumors. Breast Cancer Res. 13, 308.

Bruni-Cardoso A., Augusto T.M., Pravatta H., Damas-Souza D.M. and Carvalho H.F. (2010). Stromal remodelling is required for progressive involution of the rat ventral prostate after castration: Identification of a matrix metalloproteinase-dependent apoptotic wave. Int. J. Androl. 33, 686-695.

Carvalho H.F. and Line S.R. (1996). Basement membrane associated changes in the rat ventral prostate following castration. Cell Biol. Int. 20, 809-819.

Cheng M.K. and Shearn A. (2004). The direct interaction between ASH2, a Drosophila trithorax group protein, and SKTL, a nuclear phosphatidylinositol 4-phosphate 5-kinase, implies a role for phosphatidylinositol 4,5-bisphosphate in maintaining transcriptionally active chromatin. Genetics 167, 1213-1223.

Desai K.V., Michalowska A.M., Kondaiah P., Ward J.M., Shih J.H. and Green J.E. (2004). Gene expression profiling identifies a unique androgen-mediated inflammatory/immune signature and a PTEN (phosphatase and tensin homolog deleted on chromosome 10)-mediated apoptotic response specific to the rat ventral prostate. Mol. Endocrinol. 18, 2895-2907.

Feldman B.J. and Feldman D. (2001). The development of androgen-

independent prostate cancer. Nat. Rev. Cancer 1, 34-45.

García-Flórez M., Oliveira C. A. and Carvalho H.F. (2005). Early effects of estrogen on the rat ventral prostate. Braz. J. Med. Biol. Res. 38, 487-497.

Haffner M.C., Mosbruger T., Esopi D.M., Fedor H., Heaphy C.M., Walker D.A., Adejola N., Gürel M., Hicks J., Meeker A.K., Halushka M.K., Simons J.W., Isaacs W.B., De Marzo A.M., Nelson W.G. and Yegnasubramanian S. (2013). Tracking the clonal origin of lethal prostate cancer. J. Clin. Invest. 123, 4918-4922.

Holcomb I.N., Young J.M., Coleman I.M., Salari K., Grove D.I., Li H., True L.D., Roudier M.P., Morrissey C.M., Higano C.S., Nelson P.S., Vessella R.L. and Trask B.J. (2009). Comparative analyses of chromosome alterations in soft-tissue metastases within and across patients with castration-resistant prostate cancer. Cancer Res. 69, 7793-7802.

Isaacs J.T. (1984). Antagonistic effect of androgen on prostatic cell death. Prostate 5, 545-557.

Isaacs J.T., Furuya Y. and Berges R. (1994). The role of androgen in the regulation of programmed cell death/apoptosis in normal and malignant prostatic tissue. Semin. Cancer Biol. 5, 391-400.

Jones S., Wang T.L., Shih I.M., Mao T.L., Nakayama K., Roden R., Glas R., Slamon D., Diaz L.A., Vogelstein B., Kinzler K.W., Velculescu V.E. and Papadopoulos N. (2010). Frequent mutations of chromatin remodeling gene ARID1A in ovarian clear cell carcinoma. Science 330, 228-231.

Jung S.-K., Jeong D.G., Chung S.J., Kim J.H., Park B.C., Tonks N.K., Ryu S.E. and Kim, S.J. (2010). Crystal structure of ED-Eya2: insight into dual roles as a protein tyrosine phosphatase and a transcription factor. FASEB J. 24, 560-569.

Kawamura M., Tasaki H., Misawa I., Chu G., Yamauchi N. and Hattori M.A. (2014). Contribution of testosterone to the clock system in rat prostate mesenchyme cells. Andrology 2, 225-233.

Kim S., Kettlewell J.R., Anderson R.C., Bardwell V.J., and Zarkower D. (2003). Sexually dimorphic expression of multiple doublesex-related genes in the embryonic mouse gonad. Gene Expr. Patterns 3, 77-82.

Kramer P.R. and Wray S. (2000). Novel gene expressed in nasal region influences outgrowth of olfactory axons and migration of luteinizing hormone-releasing hormone (LHRH) neurons. Genes Dev. 14, 1824-1834.

Kurita T., Wang Y.Z., Donjacour A.A., Zhao C., Lydon J.P., O'Malley B.W., Isaacs J.T., Dahiya R. and Cunha G.R. (2001). Paracrine regulation of apoptosis by steroid hormones in the male and female reproductive system. Cell Death Differ. 8, 192-200.

Kwong J., Choi H.L., Huang Y., and Chan F.L. (1999). Ultrastructural and biochemical observations on the early changes in apoptotic epithelial cells of the rat prostate induced by castration. Cell Tissue Res. 298, 123-136.

Kyprianou N. and Isaacs J.T. (1988). Activation of programmed cell death in the rat ventral prostate after castration. Endocrinology 122, 552-562.

Nakamura M., Choe S.K., Runko A.P., Gardner P.D., and Sagerström C.G. (2008). Nlz1/Znf703 acts as a repressor of transcription. BMC Dev. Biol. 8, 108

Nantermet P.V, Xu J., Yu Y., Hodor P., Holder D., Adamski S., Gentile M.A, Kimmel D.B., Harada S.-I., Gerhold D., Freedman L.P. and Ray W.J. (2004). Identification of genetic pathways activated by the androgen receptor during the induction of proliferation in the ventral prostate gland. J. Biol. Chem. 279, 1310-1322.

Nishan U., Damas-Souza D.M., Barbosa G.O., Muhammad N., Rahim, A. and Carvalho H.F. (2015). New transcription factors involved with postnatal ventral prostate gland development in male Wistar rats during the first week. Life Sci. 143, 168-173.

Nyquist M.D., Li Y., Hwang T.H., Manlove L.S., Vessella R.L., Silverstein K.A.T., Voytas D.F. and Dehm S.M. (2013). TALEN-engineered AR gene rearrangements reveal endocrine uncoupling of androgen receptor in prostate cancer. Proc. Natl. Acad. Sci. USA 110, 17492-17497.

Palanisamy N., Ateeq B., Kalyana-Sundaram S., Pflueger D., Ramnarayanan K., Shankar S., Han B., Cao Q., Cao X., Suleman K., Kumar-Sinha C., Dhanasekaran S.M., Chen Y.B., Esgueva R., Banerjee S., Lafargue C.J., Siddiqui J., Demichelis F., Moeller P., Bismar T.A., Kuefer R., Fullen D.R., Johnson T.M., Greenson J.K., Giordano T.J., Tan P., Tomlins S.A., Varambally S., Rubin M.A., Maher C.A. and Chinnaiyan A.M. (2010). Rearrangements of the RAF kinase pathway in prostate cancer, gastric cancer and melanoma. Nat. Med. 16, 793-798.

Palevitch O., Abraham E., Borodovsky N., Levkowitz G., Zohar Y. and Gothilf Y. (2009). Nasal embryonic LHRH factor plays a role in the developmental migration and projection of gonadotropin-releasing hormone 3 neurons in zebrafish. Dev. Dyn. 238, 66-75.

Ramberg H., Alshbib A., Berge V., Svindland A. and Taskén K.A. (2011). Regulation of PBX3 expression by androgen and Let-7d in prostate cancer. Mol. Cancer 10, 50.

Rosa-Ribeiro R., Barbosa G.O., Kühne F. and Carvalho H.F. (2014a). Desquamation is a novel phenomenon for collective prostate epithelial cell deletion after castration. Histochem. Cell Biol. 141, 213-220.

Rosa-Ribeiro R., Nishan U., Vidal R.O., Barbosa G.O., Reis L.O., Cesar C.L. and Carvalho H.F. (2014b). Transcription factors involved in prostate gland adaptation to androgen deprivation. PLoS One 9, e97080.

Shabsigh A., Chang D.T., Heitjan D.F., Kiss A., Olsson C.A., Puchner P.J. and Buttyan R. (1998). Rapid reduction in blood flow to the rat ventral prostate gland after castration: Preliminary evidence that androgens influence prostate size by regulating blood flow to the prostate gland and prostatic endothelial cell survival. Prostate 36, 201-206.

Silva J.A.F., Bruni-Cardoso A., Augusto T.M., Damas-Souza D.M., Barbosa G.O., Felisbino S.L., Stach-Machado D.R. and Carvalho H.F. (2018). Macrophage roles in the clearance of apoptotic cells and control of inflammation in the prostate gland after castration. Prostate 78, 4-9.

Slorach E.M., Chou J. and Werb Z. (2011). Zeppo1 is a novel metastasis promoter that represses E-cadherin expression and regulates p120-catenin isoform expression and localization. Genes Dev. 25, 471-484.

Sunkel B. and Wang, Q. (2014). Looking beyond androgen receptor signaling in the treatment of advanced prostate cancer. Adv. Androl. 2014, 1-9.

Tomlins S.A. Rhodes D.R., Perner S., Dhanasekaran S.M., Mehra R., Sun X.-W., Varambally S., Cao X., Tchinda J., Kuefer R., Lee C., Montie J.E., Shah R.B., Pienta K.J., Rubin M.A. and Chinnaiyan A.M. (2005). Recurrent fusion of TMPRSS2 and ETS transcription factor genes in prostate cancer. Science 310, 644-648.

Wesley-Clark S., Fee B.E. and Cleveland J.L. (2002). Misexpression of

the eyes absent family triggers the apoptotic program. J. Biol. Chem. 277, 3560-3567.

Yuan X., Cai C., Chen S., Chen S., Yu, Z. and Balk S.P. (2014). Androgen receptor functions in castration-resistant prostate cancer and mechanisms of resistance to new agents targeting the androgen axis. Oncogene 29, 2815-2825.

Zhang L., Yang N., Huang J., Buckanovich R.J., Liang S., Barchetti A., Vezzani C., O'Brien-Jenkins A., Wang J., Ward M.R., Courreges M.C., Fracchioli S., Medina A., Katsaros D., Weber B.L. and Coukos G. (2005). Transcriptional coactivator Drosophila eyes absent homologue 2 is up-regulated in epithelial ovarian cancer and promotes tumor growth. Cancer Res. 65, 925-932.

Accepted March 26, 2019